Wang, L. and Chen, Q. 2008. "Evaluation of some assumptions used in multizone airflow network models" *Building and Environment, 43(10), 1671-1677.*

Evaluation of some assumptions used in multizone airflow network models

Liangzhu (Leon) Wang and Qingyan Chen*

School of Mechanical Engineering, Purdue University, 585 Purdue Mall, West Lafayette, IN 47907-2088, USA

*Tel.: +1 7654967562; fax: +1 7654967534.
E-mail address: yanchen@purdue.edu

Abstract

Multizone airflow network models assume that in a zone air temperature and contaminant concentrations are uniform, and air momentum effects are neglected. These assumptions could cause errors for airflow with strong buoyancy, large contaminant concentration gradient, or strong momentum. This study has found the correlations of the errors and some dimensionless air parameters. The assumption of uniform air temperature is acceptable when the dimensionless temperature gradient is smaller than 0.03. The assumption of uniform contaminant concentration is valid if the corresponding Archimedes number for the source zone is greater than 400. The assumption of neglecting air momentum effect is reasonable when the jet momentum effect is dissipated before reaching an opening in downstream.

Keywords: Air distribution; Multizone airflow model; Well-mixing assumption; Dimensional analysis; Contaminant transport

Nomenclature

A	Horizontal cross-sectional area of the zone/room, which contains the heat source, m^2
A_c	gross area of the inflow opening, m^2
Ar	Archimedes number
$\overline{C}$	volumetric averaged contaminant concentration
C_d	discharge coefficient of the inflow opening
C_i	contaminant concentration at a sample cell/point i
C_p	heat capacity at constant pressure, kJ/kg·K

F_{mixing}	volumetric airflow rate predicted by using well-mixing assumption, m^3/s
F_{exp}	measured volumetric flow rate, m^3/s
F_{in}	volumetric inflow rate, m^3/s
g	acceleration of gravity, m/s^2
Gr	Grashof number
h	height from the inflow opening to the outflow opening, m
K	proportionality constant
L	characteristic length of the room in m, which equals to $V_{room}^{1/3}$
L_{max}	maximum throw length of an air jet
N	total number of the sample cells
Q	volumetric inflow rate, m^3/s
Q_{in}	total heat input, W
Re	Reynolds number
R_{fa}	ratio of free area to gross area of the inflow opening
ΔT	temperature difference between the top and bottom air, Kelvin
T_{av}	averaged zone air temperature, Kelvin
T_b	air temperature at the bottom of the zone, Kelvin
T_t	air temperature at the top of the zone, Kelvin
U_c	characteristic velocity
V_i	volume of sample cell i
V_{room}	total volume of the room, m^3
Greek letters	
β	volumetric thermal expansion coefficient, K^{-1}
υ	kinematic viscosity of the air, m^2/s
ρ	air density, kg/m^3
τ	dimensionless temperature gradient

1. Introduction

Multizone airflow network models (hereafter multizone models) calculate airflow and contaminant transport between rooms in a building and between the building and outdoors. The rooms in the building are typically represented as zones, which are interconnected by airflow paths with user-defined leakage characteristics [1]. The multizone models can calculate the airflow and contaminant transport within minutes or even seconds on a PC. Validation studies by Haghighat and Megri [2], Upham [3], and Emmerich [4] showed that the multizone models could provide good predictions of building air infiltration and contaminant transport under well-mixed conditions. Therefore, the multizone models have been widely used in designs of air distribution

system, indoor air quality analyses, smoke controls, and building pressurization tests, etc. The simulated building type includes residential [5,6], commercial [7], and industrial buildings [8].

However, to achieve a fast computing speed, well-mixing assumptions in each zone are used [9]. The assumptions are uniform distributions of air temperature and contaminant concentrations in each room and neglect of air momentum effect from an inflow opening. The well-mixing assumptions could be problematic for cases with poorly mixed air and contaminants. Schaelin et al. [10] and Upham [3] pointed out that the well-mixing assumptions neglected the impacts of the local variables near the flow paths on multizone model predictions. Consequently, the results of multizone models could be inaccurate, especially for calculations of contaminant dispersions. Clarke [11] also noted that current multizone airflow models have significant limitations because momentum effects are neglected, intra-room airflow and temperature distribution cannot be determined. Gao and Chen [12] found that multizone models produce incorrect flow results due to the neglect of preserved momentum within a zone. Although these previous studies recognized the problems caused by the multizone assumptions, they did not quantitatively analyze the errors caused by the assumptions.
This paper proposes to study the errors by dimensional analysis. A few dimensionless numbers are defined to characterize the mixing levels of air temperature and contaminants as well as the importance of air momentum in a zone. By using published data in the literature, this study tries to find the correlations between the dimensionless numbers and the errors caused by the multizone assumptions. Critical values of the dimensionless numbers are provided to determine when the following multizone assumptions become invalid:

- uniform distribution of air temperature,
- uniform distribution of contaminant concentration, and
- neglect of air momentum effect.

2. Uniform distribution of air temperature

Since most multizone models do not calculate energy balance, a uniform temperature is manually specified for each zone. When the thermal buoyancy in a zone is strong, such as room with displacement ventilation or under-floor air distribution systems and rooms with water heating systems, the multizone model could not consider the impact of air temperature gradient in a zone.

The importance of air temperature gradient in a zone can be illustrated by the experimental results from Zohrabian et al. [13], who conducted a series of measurements of buoyancy-driven airflows between the two compartments in a stairwell, as shown in Fig. 1. The stairwell had one inlet and one outlet through which the buoyancy generated from a heater drove the airflow through the stairwell. This investigation used a multizone program, CONTAM [14], to calculate the airflow rate through the stairwell. As shown in

Table 1, the computed and measured data differ as much as 38% when the stairwell was modeled as a single zone by multizone method. The reason is that the large vertical air temperature gradients were not considered in the calculations. Clearly, the mixing assumption is not acceptable. Although it is possible to improve the multizone results by dividing the stairwell into upper and lower zones, it is hard to simulate two-way flows at the throat section by multizone method. Therefore, this study did not focus on improving multizone simulations but rather on finding the errors associated with the well-mixing assumption of multizone method.

Wang and Chen [15] also measured buoyancy-driven flows in a symmetric four-zone chamber as shown in Fig. 2. A heated box was placed in zone 2 and a non-heated box of the same size was symmetrically placed in zone 3. Because zone 2 had a higher air temperature than zone 3 due to the heat source, the buoyancy effect created a higher flow into zone 2 than zone 3. Table 2 compares the measured and computed airflow rate ratio between openings 1 and 2. Since the air temperature gradient in zone 2 was only 4 K for the case with 600 W heat source and 6 K with 900 W, the difference between the computed and measured flow rate is less than 10%. The mixing assumption is acceptable for this case.

Then the question is how to describe quantitatively the temperature gradient to be acceptable or unacceptable. Let us use a generic buoyancy-driven flow as shown in Fig. 3 to define the air temperature gradient in the zone as

$$\frac{\Delta T}{T_{\mathrm{av}}} = \frac{\left|T_{\mathrm{t}} - T_{\mathrm{b}}\right|}{T_{\mathrm{av}}}, \tag{1}$$

T_{av} is an input parameter for a simulation using multizone network model. For example, T_{av} is the designed room temperature for a mechanically ventilated zone/room. When T_{av} is not a designed value, T_{av} has to be determined as for a multizone simulation.

The smaller the $\Delta T/T_{\mathrm{av}}$, the better mixing of the air. A dimensionless temperature gradient, τ, can be further defined by using Reynolds number and Stanton number [16].

$$\tau = Re^{1/3} St^{2/3} \propto \frac{\Delta T}{T_{\mathrm{av}}}, \tag{2}$$

with

$$Re = \frac{F_{\mathrm{in}}}{L\upsilon}, \tag{3}$$

$$St = \frac{Q_{\text{in}}}{\rho C_{\text{p}} T_{\text{av}} A (gh)^{1/2}}, \tag{4}$$

A in Equation (4) is the horizontal cross-sectional area of a zone/room. For example, it is the horizontal cross-sectional area of zone 2 in Fig. 2. If the zone/room has partitions so that the room should be divided into sub-zones in a multizone simulation, A in Equation (4) should be the horizontal cross-sectional area of the sub-zone containing the heat source.

The τ can be quantitatively correlated to the error caused by the well-mixing assumption. If the error is defined as

$$\text{Error} = \left| \frac{F_{\text{mixing}} - F_{\text{exp}}}{F_{\text{exp}}} \right|, \tag{5}$$

By using the experimental data from the literature (the stairwell case from Zohrabian et al. [13], the four-zone chamber from Wang and Chen [15], and buoyancy-driven flow through a light well [25]), Fig. 4 shows the correlation between the τ and Error. Table 3 provides more detail of the correlation. If an error of less than 20% is acceptable for a multizone simulation, the corresponding τ should be less than 0.03.

3. Uniform distribution of contaminant concentration

The multizone models assume the species concentrations in each zone to be uniform, which may cause large errors for a zone containing a contaminant source. Schaelin et al. [10] showed the errors caused by the assumption of uniform contaminant concentration in a house with four openings and a contaminant source as illustrated in Fig. 5. It shows that the contaminant concentration at the exhaust and door could be very different, depending on the airflow pattern and the position of the contaminant sources. Multizone models, however, would treat the contaminant transported to the neighboring zones with the same concentration for all the openings that is 0.15 ppm.

Moreover, contaminant concentration could become even more poorly mixed for a space with physical obstructions [17], such as furniture and partitions. Fig. 6 shows a four-zone chamber with a partition in zone 1 [18]. The chamber had a non-uniform contaminant distribution in zone 1 by placing a contaminant source, which was simulated by SF_6, behind the partition. Due to the partition, the measured SF_6 concentration through opening 1 (C_1 = 0.98 ppm) was about 50 times higher than that through opening 2 (C_2 = 0.02 ppm). The multizone method predicted a mean SF_6 concentration of 0.5 ppm in zone 1.
These two cases show that the mixing of contaminant in a zone depends on contaminant

source and opening locations, air inflow and outflow, and local airflow pattern. The assumption of uniform distribution of contaminant concentration often fails for the zone containing a contaminant source [19]. However, if the contaminant source is also a heat source, the buoyancy effect may be strong enough to improve contaminant mixing in the space. Not many studies have been done on the contaminant mixing improved by buoyancy effect. Therefore, this investigation further studied the buoyancy effect on contaminant mixing.

For a generic room with a contaminant source, which is also a heat source, as shown in Fig. 7, the strength of buoyancy force, compared to inertial force, can be characterized by the Archimedes number [20]

$$Ar = \frac{Gr}{Re^{n}}, \tag{6}$$

The n is normally equal to two [21], but was considered to underestimate the inertial force for indoor air simulations [22]. Xue et al. [23] suggested the n to be 2.5. Reynolds [16] found that the air motion driven by buoyancy force could be better represented by a relation of $Gr \propto Re^{3}$. Based on these previous studies, this study uses n = 3, namely,

$$Ar = \frac{Gr}{Re^{3}}, \tag{7}$$

The Reynolds number is defined by Equation (3) and the Grashof number is

$$Gr = \frac{g\beta Q_{\mathrm{in}} L^{3}}{\rho C_{\mathrm{p}} F_{\mathrm{in}} \upsilon^{2}}, \tag{8}$$

To characterize the mixing level of contaminant in a zone, an index of contaminant non-uniformity, m, is used:

$$m = \sqrt{\frac{\sum_{\mathrm{i}=1}^{N} (C_{\mathrm{i}} - \overline{C})^{2} V_{\mathrm{i}}}{\sum_{\mathrm{i}=1}^{N} V_{\mathrm{i}}}}, \tag{9}$$

with

$$\overline{C} = \frac{\sum_{i=1}^{N} C_i V_i}{\sum_{i=1}^{N} V_i}, \quad (10)$$

The greater the non-uniformity index, the less uniform the contaminant concentration in the zone. Since the *m* is defined as the root mean square of the difference of local contaminant concentrations from the averaged concentration, it is equivalent to the error if the assumption of uniform contaminant concentration is used. To find how the buoyancy effect improves the mixing of contaminant, a correlation of $Ar \sim m$ was found by using three cases as shown in Table 4. They are non-uniform distributions of contaminant concentrations in a house [10] as shown in Fig. 5, in a four-zone chamber [15] as shown in Fig. 6, and in an office with displacement ventilation [24]. Table 4 shows that the parameters to calculate *Ar* can be obtained without running CFD simulations, although a multizone simulation may be needed to determine F_{in} when it was not defined in advance. CFD was only used to calculate the values of "*m*" for the correlation of Ar ~ m in this study, if experimental data were not available.

Fig. 8 shows that the contaminant concentration was highly non-uniform ($m = 9.7$) when the *Ar* was zero for four-zone chamber. With the increase of *Ar*, the buoyancy effect enhanced the contaminant mixing so that the non-uniformity index was less than 0.2 when *Ar* was greater than 400. If 20% is an acceptable error for multizone simulation, then the corresponding *Ar* should be greater than 400.

4. Neglect of air momentum effect

The multizone models assume that the air in a zone is quiescent or still, and the airflow through a zone does not have an impact on airflow distribution downwind. The power-law equation [14] only accounts for the pressure drop at an airflow opening. It equivalently assumes that the incoming airflow loses all its momentum right after the airflow path and become quiescent suddenly. The assumption is valid for cases with low air momentum effect through openings because it can be immediately dissipated after entering the zone, such as infiltration through small openings.
However, a strong momentum effect may be preserved. An example is shown by the study of airflow with a strong momentum effect in a modified four-zone chamber in Fig. 6 [18]. A strong momentum effect in zone 1 was created by mechanical ventilation from the air supply. After removing the partition in zone 1, the jet flow from the supply cannot be fully dissipated before reaching to opening 1 since opening 1 is directly opposite to and close to the air supply. Moreover, the jet flow would not affect opening 2, which is far away from the air supply. As a result, the momentum effect created a much larger flow through opening 1 than that through opening 2 as shown in Table 5. Due to the neglect of the air momentum effect in zone 1, a multizone model would calculate the same airflow

rate through the two openings.

Dissipation of airflow momentum effect is related to the supply airflow rate (Q), the distance from the jet opening to the outflow opening (X_d), the travel distance of the air jet (L_{max}), and the relative location of an opening to the jet flow. The effect can be analyzed by using jet theory in confined spaces. As shown in Fig. 9, a jet flow comprises a recirculation area and a jet expansion area, which can be further divided into four zones in a confined space [21]:

- Zone 1: initial zone
- Zone 2: transition zone
- Zone 3: fully developed turbulent flow
- Zone 4: degradation/dissipation zone

The jet momentum effect will have minimal impact on the airflow through the downstream opening if the opening is located

- inside the recirculation area, such as openings 2 and 3, or
- inside Zone 4 of the jet expansion zone, where maximum air velocity diminishes and the jet is almost dissipated, such as opening 1.

An opening in Zones 1-3 will be exposed to the momentum effect due to incomplete jet dissipation. Therefore, the maximum jet throw length [21], L_{max}, is a good parameter to estimate how the jet dissipation affects downstream airflow. If $L_{max} > X_d$ in Fig. 9, an opening will be affected by the jet momentum effect. The L_{max} can be calculated from

$$L_{max} = 1.13\frac{KQ}{U_c\sqrt{C_d R_{fa} A_c}}, \tag{11}$$

U_c is the characteristic velocity in Zone 4, which is normally 0.25 m/s. C_d is the discharge coefficient of the inflow opening, which ranges from 0.65 to 0.90.

Fig. 10 shows the errors caused by multizone simulation as a function of L_{max} for the six different supply rates for the four-zone chamber in Fig 6. Significant errors could be caused by the neglect of air momentum effects, when L_{max}/X_d is smaller than 1.

Note that the results presented in this paper were obtained through analyses of limited data, which may characterize certain airflows with air momentum effect, air temperature gradient, and contaminant concentration gradient for multizone network models, which assume each zone/room as a single node in an airflow network. More verification, dimensional analyses, and application of these results are necessary.

5. Conclusions

This investigation analyzed the impact of the assumptions of uniform distributions of air

temperatures and contaminant concentrations, and neglect of inflow momentum effect used in multizone airflow and contaminant simulations. The study concluded that the assumptions could cause significant errors in the following scenarios:

- For airflows with air temperature gradient in a zone, the non-dimensional temperature gradient τ is greater than 0.03.
- For airflows with contaminant concentration gradient, the Archimedes number is smaller than 400.
- For airflows with strong momentum effect preserved in a zone, the distance between the upstream and downstream openings is smaller than the maximum jet throw length from the upstream opening.

Acknowledgements

This research was supported by U.S. National Institute of Standards and Technology (NIST) through contract SB1341-04-Q-0771. The authors would like to thank Dr. A. K. Persily, Mr. G. N. Walton, Mr. W. S. Dols, and Mr. S. J. Emmerich of NIST for their valuable contributions to the research.

References

[1] Musser A. An analysis of combined CFD and multizone IAQ model assembly issues. ASHRAE Transactions 2001; 107(1): 371-382.

[2] Haghighat F and Megri AC. A comprehensive validation of two airflow models - COMIS and CONTAM. Indoor Air-International Journal of Indoor Air Quality and Climate 1996; 6(4): 278-288.

[3] Upham R. A validation study of the airflow and contaminant migration computer model CONTAM as applied to tall buildings. University Park, Pennsylvania, The Pennsylvania State University. 1997.

[4] Emmerich SJ. Validation of multizone IAQ modeling of residential-scale buildings: a review. ASHRAE Transactions 2001; 107(2): 619-628.

[5] Emmerich SJ, Persily AK and Nabinger SJ. Modeling moisture in residential buildings with a multizone IAQ program. Indoor Air 2002, Monterey, CA., 2002.

[6] Persily AK. Modeling study of ventilation, IAQ and energy impacts of residential mechanical ventilation. Gaithersburg, MD., National Institute of Standards and Technology 1998.

[7] Salemi R, Alamdari F and Fishwick PJ. Air distribution in a naturally ventilated office. CIBSE/ASHRAE Joint National Conference, Harrogate,U.K., 1996.

[8] Li Y, Chen L, Delsante A and Hesford G. CFD and multi-zone modeling of fog formation risk in a naturally ventilated industrial building. Roomvent 2000, Reading, U.K., 2000.

[9] Persily AK. Workshop on non-uniform zones in multizone network models. The Workshop on Non-uniform Zones in Multizone Network Models, Gaithersburg, MD., National Institute of Standard and Technology, 2003.

[10] Schaelin A, Dorer V, Maas Jvd and Moser A. Improvement of multizone model predictions by detailed flow path values from CFD calculations. ASHRAE Transactions 1994; 100(Part 2): 709-720.

[11] Clarke JA. Domain integration in building simulation. Energy and Buildings 2001; 33(4): 303-308.

[12] Gao Y and Chen Q. Coupling of a multi-zone airflow analysis program with a computational fluid dynamics program for indoor air quality studies. The 4th International Symposium on HVAC, Symposium on HVAC, Tsinghua University, Beijing, China, 2003.

[13] Zohrabian AS, Mokhtarzadehdehghan MR and Reynolds AJ. Buoyancy-driven airflow in a stairwell model with through-flow. Energy and Buildings 1990; 14(2): 133-142.

[14] Walton GN and Dols WS. CONTAMW 2.1 user manual. Gaithersburg, MD, USA: National Institute of Standards and Technology; 2003.

[15] Wang L and Chen Q. Validation of a coupled multizone and CFD program for building airflow and contaminant transport simulations HVAC&R Research 2007; 13(2): 267-281.

[16] Reynolds AJ. The scaling of flows of energy and mass through stairwells. Building and Environment 1986; 21(3-4): 149-153.

[17] Gadgil A, Lobscheid C, Abadie MO and Finlayson EU. Indoor pollutant mixing time in an isothermal closed room: an investigation using CFD. Atmospheric Environment 2003; 37(39-40): 5577-5586.
[18] Wang L and Chen Q. Theoretical and numerical studies of coupling multizone and CFD models for building air distribution simulations. Accepted by Indoor Air 2006.
[19] Yuan J and Srebric J. Improved prediction of indoor contaminant distribution for entire buildings. The 2002 ASME International Mechanical Engineering Congress and Exposition, New Orleans, Louisiana, USA, 2002.
[20] Incropera FP and DeWitt DP. Fundamentals of heat and mass transfer. Hoboken, NJ: John Wiley; 2007.
[21] ASHRAE. ASHRAE Handbook of Fundamentals: American Society of Heating, Refrigerating and Air-Conditioning Engineers; 2005.
[22] Zhang JS, Wu GJ and Christianson LL. A new similitude modeling technique for studies of non-isothermal room ventilation flows. ASHRAE Transactions 1993; 99(1): 129-138.
[23] Xue, H., Hihara, E., Saito and T. Temperature stratification of heated airflow in a fire tunnel. Jsme International Journal Series B-Fluids and Thermal Engineering 1994; 37(1): 187-194.
[24] Srebric J, Chen Q and Glicksman LR. Validation of a zero-equation turbulence model for complex indoor airflows. ASHRAE Transactions 1999; 105(2): 414-427.
[25] Kotani H, Satoh R and Yamanaka T. Natural ventilation of light well in high-rise apartment building. Energy and Buildings 2003; 35(4): 427-434(8).

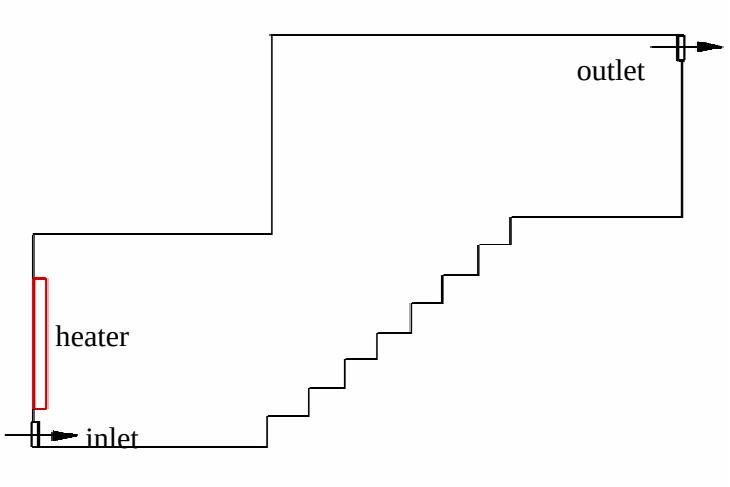

Fig. 1. Schematic diagram of the stairwell model [13].

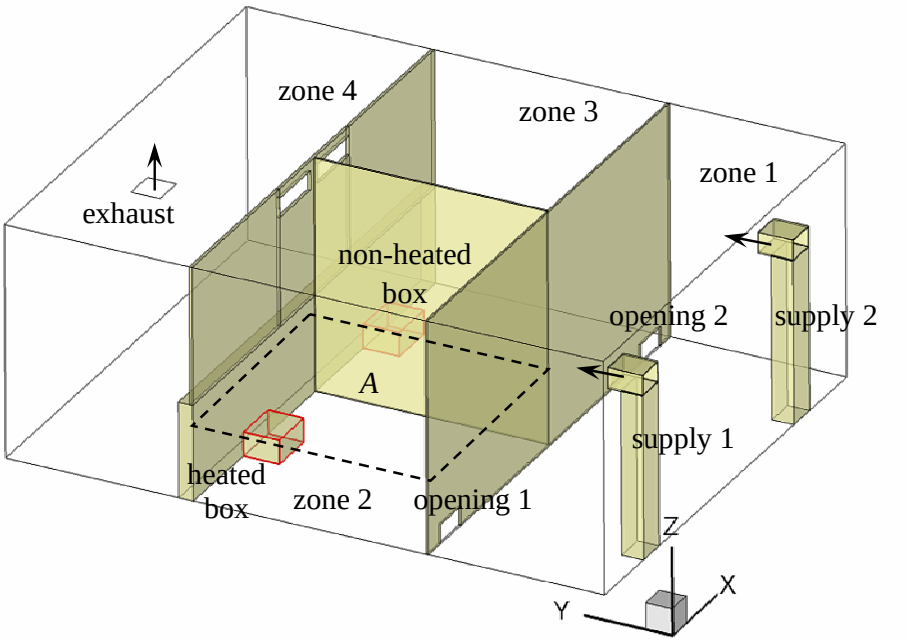

Fig. 2. Schematic of a four-zone chamber used for studying non-uniform air temperature distribution [15]

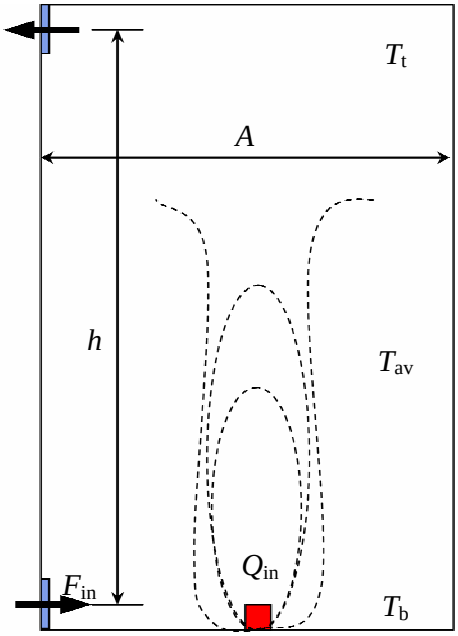

Fig. 3. Air temperatures in a room with generic buoyancy-driven flow

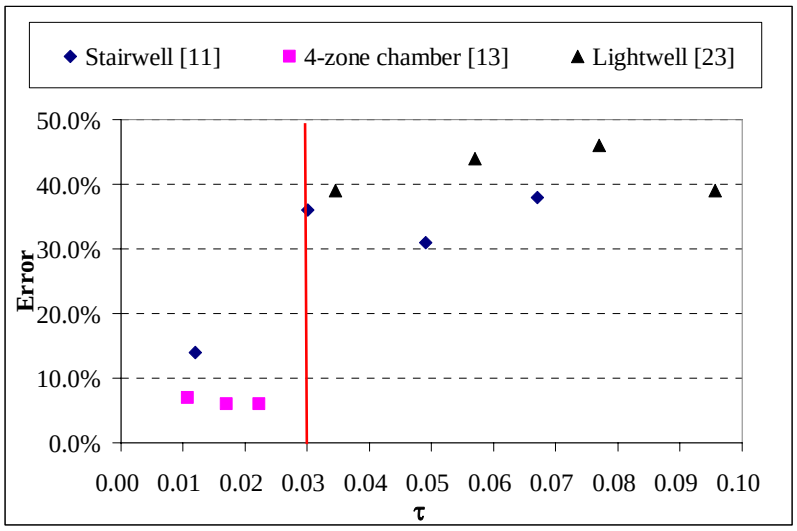

Fig. 4. The simulation errors as a function of the dimensionless air temperature gradient for different buoyancy-driven flows

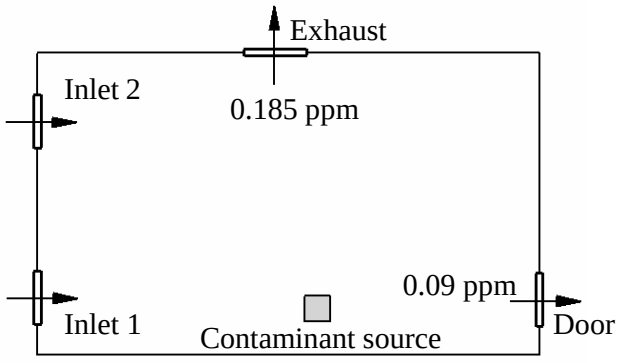

Fig. 5. Contaminant concentrations in a house from a CFD simulation [10].

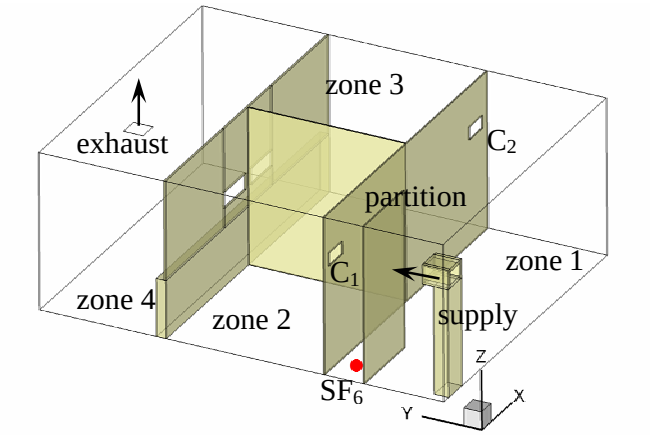

Fig. 6. The layout of a four-zone chamber used for studying non-uniform contaminant concentration distribution, when zone 1 is with the partition, and for studying airflow with strong momentum effect, when zone 1 is without the partition [15]

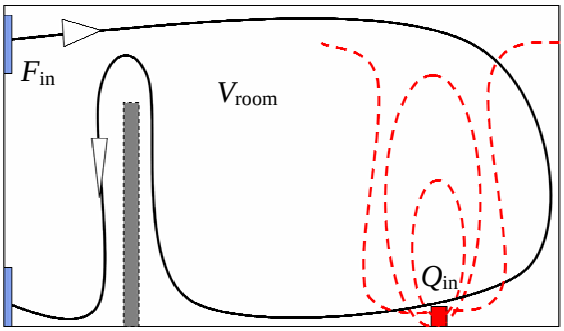

Fig. 7. Contaminant transport enhanced by buoyancy effect in a generic room with an internal partition

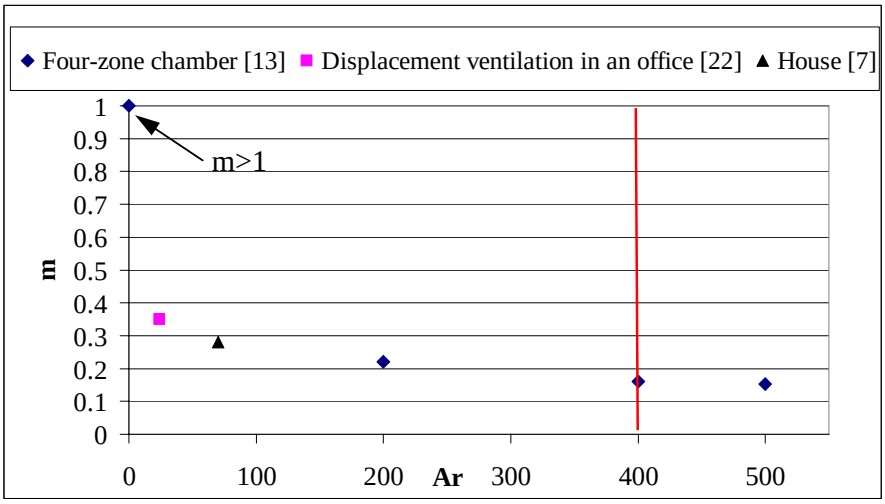

Fig. 8. The non-uniform index, m, as a function of Ar for different cases with non-uniform contaminant concentration distributions

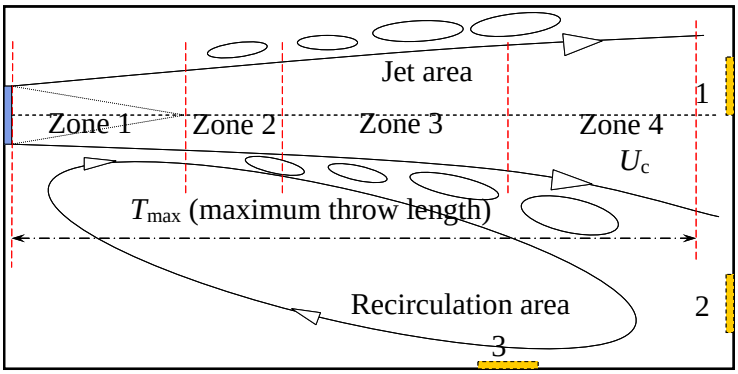

Fig. 9. Illustration of a jet airflow in a confined space

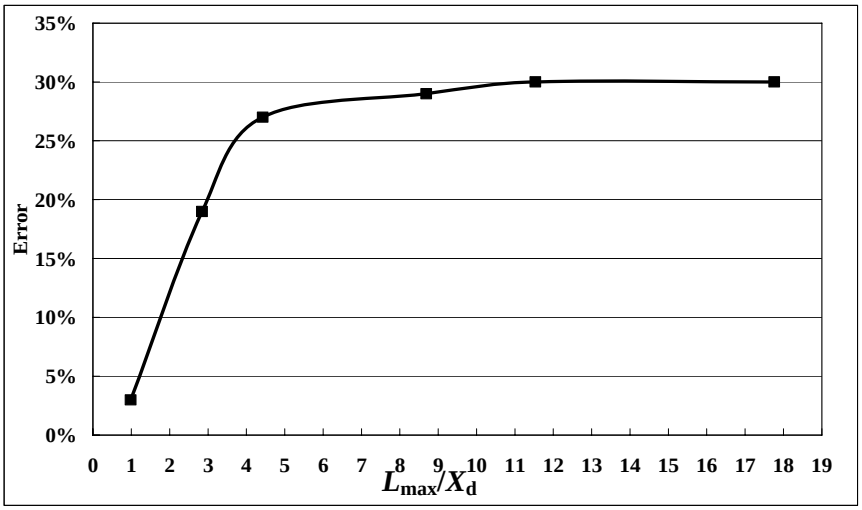

Fig. 10. The simulation errors as a function of L_{max}/X_d for different momentum strengths

Table 1

Comparison of measured and computed airflow rates for the stairwell case

Case	A	B
Heating power from the heater, Q_{in} (W)	300	900
Measured mean air temperature (°C)	29.6	40.4
Measured vertical air temperature gradient (K)	7	17
Measured airflow rate ($\times 10^3$ kg/s)	4.48	7.22
Computed airflow rates by using the well-mixing assumption ($\times 10^3$ kg/s)	2.85	4.49

Table 2

Comparison of measured and computed airflow rates for the four-zone chamber with different heating power

Case	A	B
Heating power from the heated box, Q_{in} (W)	600	900
Measured vertical air temperature gradient in zone 2 (K)	4	6
Measured airflow rate through opening 1 over that through opening 2	1.32	1.45
Computed airflow rate through opening 1 over that through opening 2	1.24	1.36

Table 3

Important parameters for the three non-uniform temperature cases and the errors caused by the well-mixing assumption

Cases	τ	Q_{in} (w)	F_{in} ($\times 10^2$ m^3/s)	L (m)	A (m^2)	h (m)	T_{av} (K)	Error
Stairwell (Fig. 1) [13]	0.015	100	0.24	1.43	0.46	2.43	299	14%
	0.035	300	0.37	1.43	0.46	2.43	303	36%
	0.061	600	0.52	1.43	0.46	2.43	311	31%
	0.083	900	0.60	1.43	0.46	2.43	313	38%
Four-zone chamber (Fig. 2) [15]	0.011	300	5.8	2.45	6.01	2.44	296	7%
	0.017	600	5.8	2.45	6.01	2.44	298	6%
	0.022	900	6.0	2.45	6.01	2.44	300	6%
Light well [25]	0.035	10	0.035	0.2	0.02	0.48	299	39%
	0.057	20	0.042	0.2	0.02	0.48	307	44%
	0.077	30	0.048	0.2	0.02	0.48	313	46%
	0.096	40	0.054	0.2	0.02	0.48	322	39%

Table 4

Important parameters for the three cases with non-uniform contaminant concentrations and the errors caused by the well-mixing assumption

Cases		*Ar*	Q_{in} (w)	F_{in} (m^3/s)	*L* (m)	*m*
House [10] (Fig. 5)	CFD simulation	70	500	0.07	4.2	28%
Four-zone chamber [15] (Fig. 6)	Experiment	0	0	0.1	2.22	9.7
	CFD simulation	200	400	0.02	2.22	22%
		400	810	0.02	2.22	16%
		500	1000	0.02	2.22	15%
Displacement ventilation in an office [24]	Experiment	24	173	0.05	3.5	35%

Table 5

Comparison of measured and computed airflow rates for the four-zone chamber with different supply flow rates

Air supply (m^3/s)	Ratio of airflow rate through opening 1 over that through opening 2	
	Experiment	Multizone simulation with the well-mixing assumption
0.034	1.6	1.0
0.053	2.2	1.0
0.105	2.4	1.0
0.140	2.5	1.0
0.215	2.5	1.0